UNIDIRECTIONAL HYBRID COMPOSITE OVERLOAD SENSORS

T. Rev[1*], G. Czél[2] , M. Jalalvand[1] , M. R. Wisnom[1]

[1] Bristol Composites Institute (ACCIS), University of Bristol, Queens Building, University Walk, Bristol, BS8 1TR, United Kingdom
*Email: tamas.rev@bristol.ac.uk, Web Page: http://www.bristol.ac.uk/composites/
[2]Department of Polymer Engineering, Faculty of Mechanical Engineering, Budapest University of Technology and Economics, Műegyetem rkp. 3., H-1111 Budapest, Hungary
Email: czel@pt.bme.hu , Web Page: http://www.pt.bme.hu

Keywords: Hybrid composites, Fragmentation, Delamination, Damage detection, Mechanical testing, Health monitoring

ABSTRACT

A purpose-designed, thin-ply interlayer glass/carbon hybrid composite overload sensor concept is presented, which can be used for structural health monitoring (SHM) of composite structures, with potential for safer operation in service. It has been demonstrated that the sensors work satisfactorily and the striped pattern in the composite structure gives a visual indication of overload of the substrate. An analytical model developed here allows for these sensors to be tailored to suit different substrate materials and design strains. The sensors - comprising a single layer of Ultra-High Modulus (UHM) carbon/epoxy and S-glass/epoxy material - were characterised by experimental strain measurements, and finite element analysis (FEA) regarding their accuracy and the effect of their stiffness on the utilized substrate.

1 INTRODUCTION

Composite materials play a significant role in satisfying the increasing demands of aerospace, automotive, high-end sports industries as well as civil engineering and leisure equipment. These applications require high stiffness and strength, enhanced chemical and corrosion resistance, good fatigue properties and most importantly weight savings. However, the incorporation of such materials is limited by their inherent brittleness as they often fail in a catastrophic manner, without preceding detectable damage or warning. To overcome this limitation and to avoid the utilization of over-conservative design envelopes and large safety margins, a new Structural Health Monitoring (SHM) concept is introduced here. While monitoring structural integrity, especially during visual inspection, damage detected in time can not only prevent catastrophic failure but it can also indicate the need for further, more thorough non-destructive testing (NDT). A UK patent application by Czél et al. [1] based on a unique feature of a purpose designed unidirectional (UD) hybrid composite allows for visual overload indication simply from a change in appearance as the composite is loaded over a predefined strain value. The aim of this paper is to prove this novel concept and to characterise and optimize the sensing characteristics of such technology by a simple analytical and finite element (FE) model and mechanical testing.

2 SENSING MECHANISM

A unidirectional hybrid composite sensor is generally comprised of glass/epoxy and carbon epoxy materials. The composite is attached to a substrate/component, and the originally intact carbon layers absorb the incident light passing through the translucent glass layer, exhibiting a dark appearance as illustrated in Figure 1 (a). After exceeding the failure strain of the 'sensing' carbon layer, the incident light is reflected from the locally damaged glass/carbon interface resulting in the appearance of light stripes around the cracks in the carbon layer as seen in Figure 1 (b).

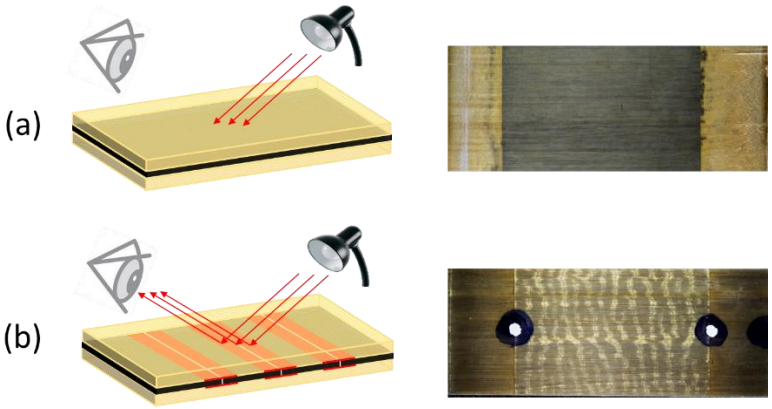

Figure 1. The sensing mechanism behind the unidirectional strain overload sensors: (a) intact carbon layers absorbing light at glass/carbon interface (b) striped pattern visible due to light being reflected from the locally damaged glass/carbon interface.

The interfacial damage is caused by the fragmentation of the carbon fibre reinforced sensing layer followed by stable and dispersed delamination as previously demonstrated by Czél et al [2]. This also produced pseudo-ductile behaviour, and was achieved by combining unidirectional standard thickness glass/epoxy and thin ply carbon/epoxy plies to create inter-laminar hybrid composites [3]. Czél et al. have observed that the translucency of the glass/epoxy plies in these hybrids allows the cracks in the carbon layer to be visible with the naked eye. Based on the failure mechanism of such thin-ply hybrids, two different types of pattern can be differentiated. One of them represents a single fracture of the low-strain material followed by sudden, unstable delamination [4] whilst the other one is fragmentation of the low-strain material followed by gradual, dispersed delamination [2]. These two distinct failure mechanisms which can both be used for sensing overloads are illustrated in Figure 2.

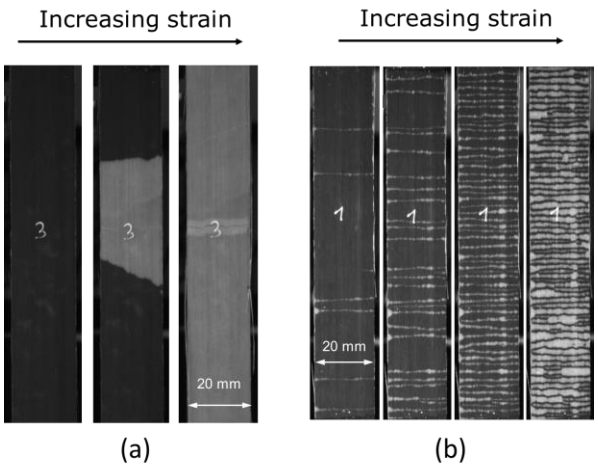

Figure 2. Visual patterns based on different failure mechanisms of thin-ply glass/carbon hybrids: (a) carbon layer fracture followed by sudden delamination (b) carbon layer fragmentation followed by stable, dispersed delamination

3 EXPERIMENTAL

3.1 Specimen and sensor geometry, configuration

The design of this preliminary study builds on the work carried out by Czél et al. [2] who demonstrated a series of new material combinations exhibiting favourable pseudo-ductile stress-strain responses. The glass/carbon reinforced hybrid composite material configuration proposed here is a suitable system for the fabrication of the aforementioned overload sensors, mainly designed for tensile load dominated applications.

The side and top view schematic of the specimens are illustrated in Figure 3. The grey areas (L_s) represent the carbon sensing layer situated beneath the translucent glass layer. Each specimen is comprised of the substrate laminate with a sensor laminate in the central section on one side, where L_f / L_s / L_t / t_s / w are the free length / sensing layer length / sensor total length / substrate thickness / and specimen width respectively. The sensor laminate comprises one thin layer of ultra-high modulus (UHM) UD carbon/epoxy and a standard thickness ply of UD S-glass/epoxy prepreg material. The substrate laminate comprises 15 standard thickness plies of UD intermediate modulus (IM) IM6 carbon/epoxy material supplied by Cytec. All applied prepregs have similar cure temperature (in the 120 °C range) and are suitable for curing together in an autoclave. The basic material data of the applied fibres and prepreg systems can be found in Table 1 and Table 2.

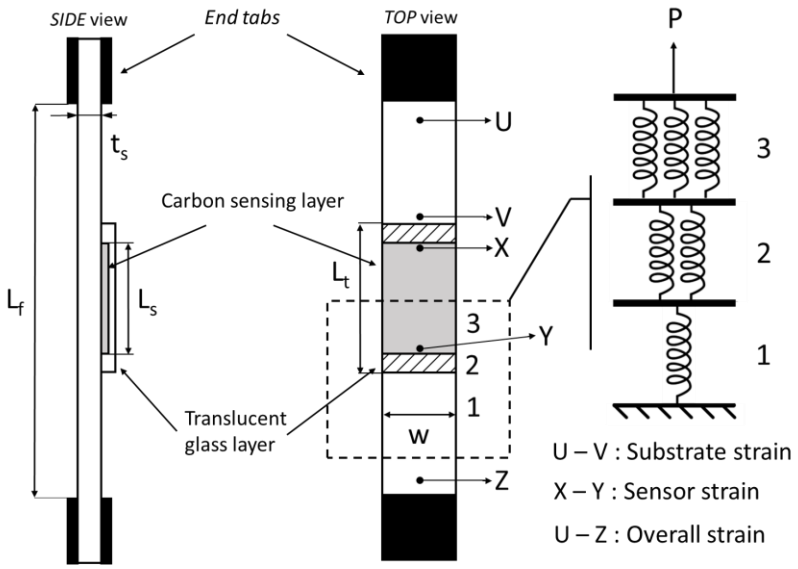

Figure 3. Schematic of the (a) side and (b) top view of an unidirectional tensile specimen equipped with a hybrid composite overload sensor, (c) illustrates a simple elastic stiffness model representing the behaviour of the unidirectional laminate

The nominal dimensions of the specimens were 260/160/20/2.4 mm overall length/free length/width/substrate thickness respectively and the nominal dimensions of the sensors were 50/30 mm total length (L_t) sensor length (L_s) respectively.

Table 1. Fibre properties of the applied unidirectional prepregs based on manufacturers data (carbon fibre types: IM – intermediate modulus, UHM – ultra high modulus)

Fibre type	Elastic modulus [GPa]	Density [g/cm^3]	Strain to failure [%]	Tensile strength [GPa]
UHM carbon	780	2.17	0.5	3.43
Hextow IM6 carbon	279	1.76	1.9	5.72
S-glass	88	2.45	5.5	4.8-5.1

Table 2. Cured ply properties of the applied unidirectional prepregs

Prepreg type	Areal density[1] [g/m^2]	Cured ply thickness[2] [µm]	Fibre volume fraction[2] [%]	Initial elastic modulus[2] [GPa]	Tensile strain to failure[3] [%]
UHM carbon/epoxy	63	63	46.5	364.4	0.48 [2]
IM6/950 carbon/epoxy	135	153	50	141.2	1.8[2]
S-glass/913 epoxy	190	155	51	45.6	3.9

[1]Based on manufacturers data
[2]Calculated using manufacturers data
[3]Based on measurements

3.3 Manufacturing

The specimens were manufactured by co-curing the sensor and substrate laminates together. These laminates were fabricated by a conventional process that is used for prepreg composite manufacturing: hand lay-up followed by standard vacuum bagging on a flat aluminium tool plate. Additional silicone sheets were placed on top of the laminates in order to ensure a smooth top surface and an even pressure distribution. Following layup, the laminates were cured in an autoclave. The highest cure temperature and longest cure time of all the constituent prepregs' individual cure cycles have been used to ensure full cure for all the material systems and the highest mechanical performance. The cycle used was 155 mins@137 °C, with 0.7 MPa applied pressure and a temperature ramp up rate of 2°C/min. The tensile specimens were fabricated by a diamond cutting saw. Untapered, 1.7 mm thick end-tabs made of a balanced glass fibre fabric reinforced composite laminate were bonded to the specimens using a commercially available Araldite 2014/1 type two-part epoxy system. The coupons were then put into an atmospheric oven to cure the adhesive for 120 mins@80 °C.

3.4 Test procedure

Mechanical testing was carried out on an INSTRON 8801 100 kN rated, computer controlled, universal servo-hydraulic test machine with wedge type hydraulic grips under uniaxial tensile loading and displacement control at a crosshead speed of 1 mm/min. The clamping pressure was kept at 2000 psi in order to avoid slippage of the specimens in the grips. Various local (sensor) and global strains were measured using an Imetrum video extensometer system, with the test machine outputting the corresponding force signals. The high-definition extensometer videos recorded during the tests were kept for determining the first fracture (fragmentation) of the carbon sensing layer by visual inspection.

3.5 Results and discussion

Figure 4 shows the stress-strain response of a tensile specimen fitted with a unidirectional hybrid sensor comprising single plies of UHM carbon/epoxy and S-glass/epoxy prepregs. Substrate strain (defined between points of U and V in Figure 3) represents the surface strain of the substrate only, overall strain (defined between points of U and Z in Figure 3) represents the overall extension measured along the free length of the specimen, while sensor strain (defined between points of X and Y in Figure 3) shows the surface strain of the sensor. The red dashed and continuous lines illustrate the strain and stress respectively at which the first sensing layer fracture occurred in the sensor. The stress and strain values were determined from the logged data based on visually inspecting the videos recorded during testing and extracting the time for the first visible fracture of the sensing layer. The summary of the test results is given in Table 3.

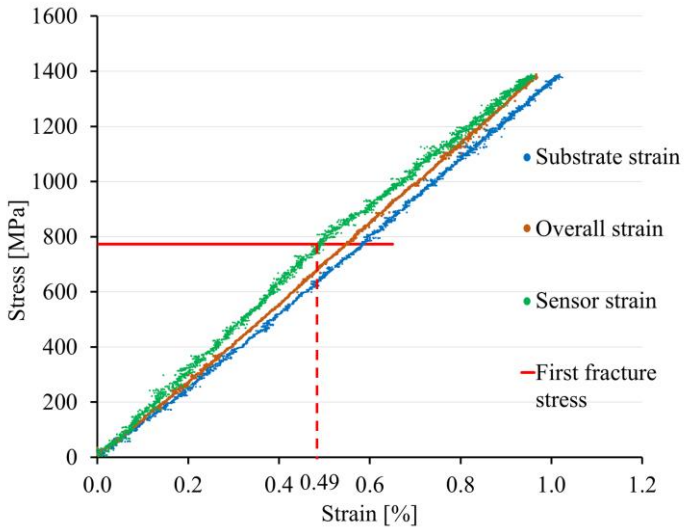

Figure 4. Typical stress-strain response of a tensile specimen fitted with a UD hybrid sensor

Table 3. Comparison of test results to that of the analytical model

Substrate/ Sensor configuration	No. of specimens tested	Sensor strain at first crack in sensor layer [%] (CV [%])	Substrate strain at first crack in sensor layer [%] (CV [%])	Substrate stress at first crack in sensor layer [MPa] (CV [%])
$IM6_{15}$/UHM carbon/ S-glass	5	0.52 (3.27)	0.62 (4.55)	820 (5.16)
Analytical model	-	0.57	0.62	805

The stress-strain curves of Fig. 4 clearly show how the overall stiffness of the specimen has been increased due to the integration of a sensor. The average apparent modulus of the specimens at the section where the sensor is placed (measured between points X and Y) is 155 GPa, while the measured substrate modulus from nominal thickness is only 138.5 GPa. This stiffening effect shows that the trigger strain of the sensors has to be corrected for the actual substrate stiffness to represent the strain in the free-standing substrate. Furthermore, it should be noted that the sensor strain curve above also reflects the damage-induced non-linear behaviour of the specimen-sensor system.

To assess the effect of the UD composite sensors on the stiffness of the substrate material and to estimate the strain distribution along the length of the specimens, a simple elastic analytical model was set up. This preliminary strain data gives an estimate of the 'accuracy' of the composite strain sensors (especially to what extent the strain at the first sensor crack agrees with the measured substrate strain) and whether they need to be calibrated. The input parameters of the model include the moduli of the prepreg materials, cured ply thicknesses (CPTs), lay-up (the number of plies), the length and width of the coupons as well as the applied uniaxial tensile load.

The equivalent stiffness model as seen in Figure 3 (c), determines average strains based on calculating an effective stiffness for a certain section of the specimen using simple series and parallel rules that connect the distinct materials. The numbered regions on the figure represent areas consisting of (1) substrate material only, (2) the outermost glass/epoxy layer + substrate material and (3) glass/epoxy +UHM carbon sensing layer + substrate material. This analytical model does not take through thickness strain variation into consideration as it is a pure tensile model not accounting for asymmetry induced bending.

It gives a rough estimate of the error of these UD hybrid sensors which is defined as the difference between the average sensor strain (calculated between points X and Y on Figure 3) and the average strain calculated in a section where there is substrate material only (defined between points U and V on Figure 3).

The sensor extension measured at the first crack appearance in the sensor layer (0.52%, see Table 3.) is close to the failure strain of the UHM carbon fibres (see Table 1). Additionally, a strain mismatch can be observed between the measured sensor and substrate strains. This is underpinned by the calculations made by the analytical stiffness model (described above). This comparison highlights the difference between the predicted values and real measurements. While the calculated sensor strain (0.57%) shows a large deviation from the measured sensor strain, the substrate strain matches with the experimental value. It is due to the analytical model not taking the through-thickness strain variation due to asymmetry into account. In the section of the specimen where the sensor is placed, the mismatch between the experimental surface strain and the analytical strain (which reflect the predicted mid-plane strain) is high because the cross-section is asymmetric there. On the other hand the predicted substrate strain matches well with the measured one because the cross-section is symmetric where there is no sensor, so the strain is not expected to vary across the thickness. The analytical model was run with 40.3 kN tensile load corresponding to the load at which the first cracks were detected in the sensor during the real experiments.

A finite element model (FEM) was also set up in a commercial software package (Abaqus). The finite element analysis (FEA) incorporated a 2D shell model of the laminate along the gauge length of the specimen up until the end-tab regions. The analysis was carried out using conventional linear 4 noded S4R shell elements with the definition of linear elastic properties for the distinct materials as summarised in Table 4. There was an offset applied to certain shell elements to account for the asymmetry and different thicknesses of the different regions on the specimen as illustrated in Figure 3.

A static load case was run where the specimen was built in along one edge and loaded at the other one constraining all degrees of freedom except in the loading direction. Due to the length of the specimen the boundary conditions do not affect the stress/strain state of the sensor area.

Table 4. Linear elastic material properties utilized in the finite element model

Material	E_1 [GPa]	E_2 [GPa]	G_{12} [GPa]	ν_{12} [-]	G_{13} [GPa]	G_{23} [GPa]	ν_{23} [-]
UHM carbon/epoxy	364.57	10.9	3.71	0.31	3.7	3.7	0.45
IM6/950 carbon/epoxy	141.5	13	4.58	0.31	4.6	4.5	0.45
S-glass/epoxy	46.55	10.5	3.78	0.26	3.8	3.6	0.45

In order to compare the results of the basic analytical model (neglecting the effect of bending), and the more accurate one by the FEA - accounting for bending -, a common load case had to be set. The specimen (seen in Figure 3) was loaded with a uniaxial tensile load of 20kN (~0.3-0.4% strain). This preceded the failure strain of the UHM carbon fibres hence keeping the load case in the linear region of the stress-strain curves of Figure 4. The results were validated against strain gauge measurements. There were two specimens tested, where strain gauges were placed on the top surface of the glass layer of a co-cured sensor and on the back surface of the substrate. These gauges were placed in order to determine the distribution of strains through the thickness of the specimens at a given cross section within the sensor area. A summary of the results compared with the strain gauge measurements can be seen in Table 5.

Figure 5 shows the contour of strain output by the FEA for (a) the bottommost point of the substrate and for (b) the topmost point of the glass layer. Figure 5 (c) illustrates the comparison of through thickness strain distributions predicted by FEA and measured by the strain gauges. The graph shows the difference between the predictions and experimental values.
On the vertical axis, zero represents the bottom of the substrate/backface of the specimen.

Table 5. Summary of the strain results output by different models for a 20kN load case at the sensor area. The table shows the calculated curvatures and strain variation between the topmost and bottommost surfaces of the specimen.

Model/test method	Sensor top surface strain [%]	Substrate bottom surface strain [%]	Average through thickness strain [%]	κ curvature [1/m]	Difference between top and bottom surface strain [%]
Analytical model	0.282*	0.282*	0.282	n/a	n/a
FE model	0.260	0.303	0.282	-0.171	14
Strain gauge measurements	0.254	0.315	0.285	-0.243	19

*The analytical model outputs a constant average strain across the thickness of the specimen and the sensor

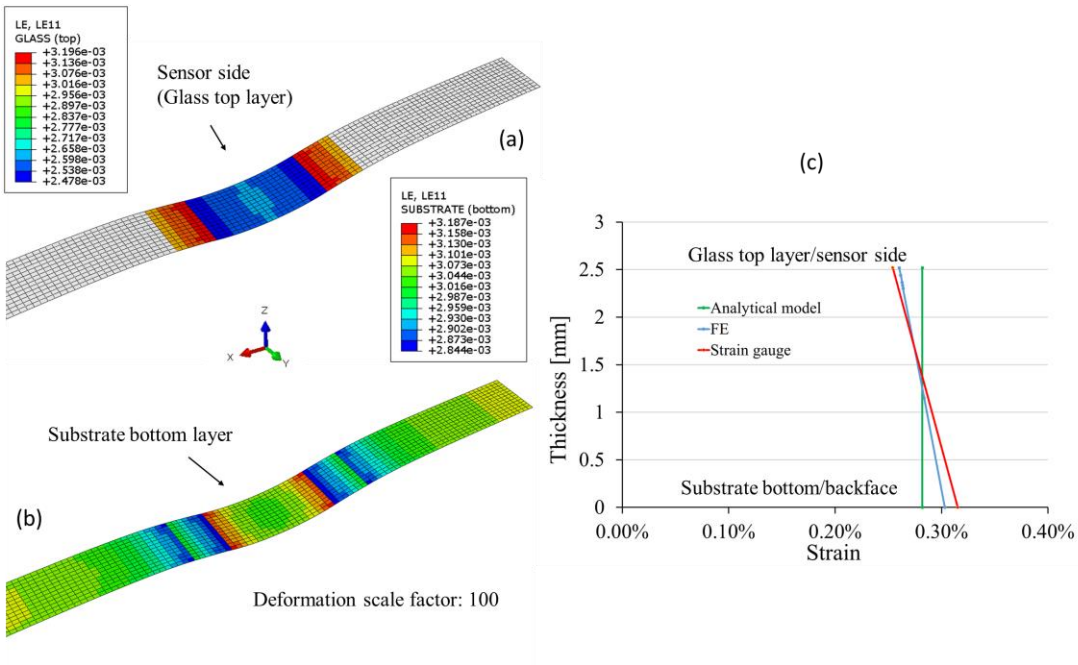

Figure 5. Contour of axial strain in the (a) topmost point of the glass layer; (b) bottommost point of the substrate (c) comparison of through-thickness strain variation by different models and strain gauge measurements.

As shown in Table 5, the strain calculated by the analytical model exhibits a large deviation from the strain gauge results. It is due to the nature of the calculation not accounting for bending, which assumes uniform strains through the thickness of the laminate. The FEA model is a lot more realistic, capturing the actual geometry and boundary conditions of the specimen with the sensor (giving the deflected shape and variation along the length).

However, the through thickness average strains are comparable: the value of the stiffness model and the FEA predictions have a deviation of only around 1% when compared to the experimental value.

The reason for the small deviation can be stemming from i) the assumptions made (material properties, boundary conditions) and ii) the accuracy of the measurement system (e.g. misalignment of gauges).

The accuracy of the sensor measurements is highly dependent on the overall stiffness of the substrate (hence on the number of constituent plies). Figure 6 illustrates the percentage error (between the substrate strain and the sensor strain) calculated by the model as a function of the substrate thickness for different grade carbon fibres.

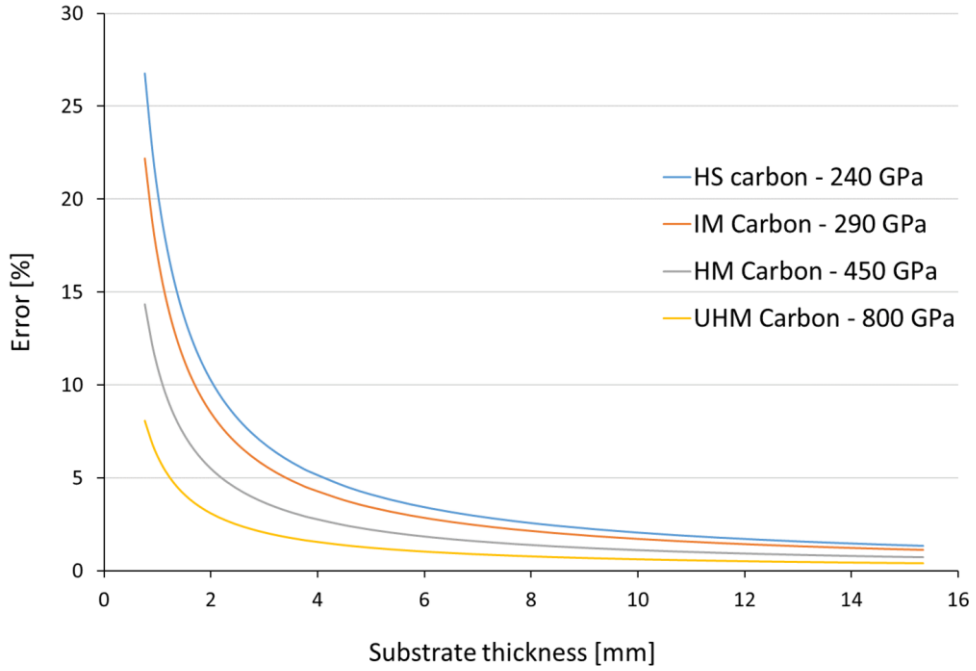

Figure 6. Accuracy of sensor strain measurement predicted by the analytical model

It can be stated that the thicker the substrate material is, the less stiffening effect the sensor has. The graph above is a useful tool for deciding whether the sensors need to be calibrated or not as a first estimate when applying it to various stiffness structures. In order to achieve an error less than 10% utilizing the presented which? carbon fibres above, a minimum substrate thickness of 2.15 mm is required. The error calculated by the model represents the difference in average strain of the UD hybrid sensors (sensor strain between points X and Y on Figure 3) and the substrate (strain between points U and V on Figure 3) discarding the effect of bending. As the strain has a relatively small variation through the thickness (the maximum is 10% higher than the midplane value), this simple model can give a reasonable indication of the extra stiffness added by the sensor and it is suitable for running parametric studies.

4 CONCLUSION

A novel Structural Health Monitoring (SHM) concept has been introduced based on purpose designed pseudo-ductile hybrid composites. It has been shown that the sensors work satisfactorily and visually indicate the overload of the substrate laminate used in this study. These robust and lightweight sensors are completely wireless and offer low-cost and simple solutions for visual overload indication. They can be applied either as a structural sensing layer or as sensors locally integrated to a component. Key design parameters are the stiffness of the sensing layer, the stiffness of the substrate material and their ratio. To investigate the stiffness effects and the accuracy of the sensors, a simple analytical model was proposed. The results of this analytical model and a more detailed Finite Element Analysis were compared against experimental strain gauge measurements on carbon/epoxy substrates fitted with overload sensors. It was shown that the FEA provides the best agreement with the experimental results in terms of sensor and substrate strain values at the first fracture of the sensing layer.

ACKNOWLEDGEMENTS

This work was funded under the UK Engineering and Physical Sciences Research Council (EPSRC) Programme Grant EP/I02946X/1 on High Performance Ductile Composite Technology in collaboration with Imperial College London. Gergely Czél acknowledges the Hungarian Academy of Sciences for funding through the János Bolyai scholarship and the Hungarian National Research, Development and Innovation Office - NKFIH for funding through grants ref. OTKA K 116070 and OTKA PD 121121. The authors acknowledge Hexcel Corporation and North TPT for supplying the materials for this research. All data required to support the conclusions are provided within the paper.

REFERENCES

[1] G. Czél, M. Jalalvand, P. Kevin, M.R. Wisnom, UK Patent Application number: 1520988.5.

[2] G. Czél, M. Jalalvand, M.R. Wisnom, Design and characterisation of advanced pseudo-ductile unidirectional thin-ply carbon/epoxy– glass/epoxy hybrid composites, Compos. Struct. 143 (2016) 362–370. doi:10.1016/j.compstruct.2016.02.010.

[3] G. Czél, M.R. Wisnom, Demonstration of pseudo-ductility in high performance glass/epoxy composites by hybridisation with thin-ply carbon prepreg, Compos. Part A Appl. Sci. Manuf. 52 (2013) 23–30. doi:10.1016/j.compositesa.2013.04.006.

[4] G. Czél, M. Jalalvand, M.R. Wisnom, Hybrid specimens eliminating stress concentrations in tensile and compressive testing of unidirectional composites, Compos. Part A Appl. Sci. Manuf. (2016). doi:10.1016/j.compositesa.2016.07.021.

[5] L. P. Kollár, G. S. Springer, Mechanics of Composite Structures.